Hindawi
Advances in Astronomy
Volume 2021, Article ID 6685578, 16 pages
https://doi.org/10.1155/2021/6685578

Research Article

A Generic Embedding Class-I Model via Karmarkar Condition in $f(\mathscr{R}, \mathbb{T})$ Gravity

M. Zubair[1], **Saira Waheed**[2] **and Hina Javaid**[1]

[1]*Department of Mathematics, COMSATS University Islamabad, Lahore Campus, Lahore, Pakistan*
[2]*Prince Mohammad Bin Fahd University, Khobar, Saudi Arabia*

Correspondence should be addressed to M. Zubair; mzubairkk@gmail.com

Received 7 November 2020; Revised 6 December 2020; Accepted 30 December 2020; Published 9 February 2021

Academic Editor: Muhammad Farasat Shamir

In the present work, we investigate the existence of compact star model in the background of $f(\mathscr{R}, \mathbb{T})$ gravity theory, where $\mathscr{R}$ represents the Ricci scalar and $\mathbb{T}$ refers to the energy-momentum tensor trace. Here, we use Karmarkar condition for the interior stellar setup so that a complete and precise model following the embedding class-I strategy can be obtained. For this purpose, we assume anisotropic matter contents along with static and spherically symmetric geometry of compact star. As Karmarkar embedding condition yields a relationship of metric potentials, therefore we assume a suitable form for one of the metric components as $e^{\phi} = ar^2 + b^{n-1}r^n + 1$, where a and b represent constants and n is a free parameter, and evaluate the other. We approximate the values of physical parameters like a, A, and B by utilizing the known values of mass and radius for the compact star Vela X-1. The validity of the acquired model is then explored for different values of coupling parameter λ graphically. It is found that the resulting solution is physically interesting and well-behaved.

1. Introduction

General relativity (GR) is regarded as the most promising theory which has extremely good compatibility with the cosmic observations. In the background of GR, the examination of structural properties and the dynamic nature of high-density compact objects like neutron stars has gained significant interest in recent decades. Pulsars and other high magnetic-field spinning stars are some of the high-density compact objects that are regarded as a major discovery in astrophysics. Because of the lack of detailed description of such objects, it is considered that the matter of these compact objects can include composite subatomic particles. Consequently, the basic problem of astrophysics is to determine the configuration and formation of the fluid distribution in the internal setup of spherical objects. The first two precise solutions of Einstein field equations depicting a stable spherically symmetric configuration are found by Schwarzschild [1, 2] which further inspired many researchers to find the exact solutions of Einstein field equations using perfect matter [3–10]. Earlier, the spherically symmetric distribution of matter was thought to be made of isotropic fluid where $p_r = p_t$. In 1992, Jeans [11] proposed the presence of anisotropy factor which highlights a deeper understanding of the distribution of matter under intense and peculiar conditions occurring within stellar objects. Ruderman [12] suggested that, at a very high density, the stars may show the anisotropic behavior where nuclear interaction is relativistic. There are several causes of anisotropy within a stellar structure like the existence of a superfluid, solid core, a combination of various liquids, phase fluctuations, magnetic field, and density [13–15]. Bowers and Liang [16] investigated the characteristics of a fluid distribution (which is relativistic anisotropic) inside static spherically symmetric configuration. The possible effects of anisotropy on the stability of compact objects were investigated by Dev and Gleiser [17–19]. They showed that the difference in pressures influences the physical properties of configuration, mass, and areas of excessive pressure. Herrera and Santos [20] explained the impact of localized anisotropy in self-gravitating objects. Moreover, this work has been extended for all feasible isotropic, anisotropic, and

charged anisotropic solutions by adopting a general procedure for the spherically symmetric metric [21, 22].

Although GR is a successful theory, it faces certain obstacles after the cosmologists unfolded the scenario of dark universe. It is argued that observational data of many experiments [23–25] is evident that the universe is expanding in its current state. This expansion was actually discovered by the two sovereign projects, namely, Supernova Cosmology Project and High-Z Supernova Search Team in 1998. This observation about the cosmological expansion of the universe has been perceived as exceptionally crucial mystery in modern physics. It is claimed that the major cause behind this expansion is the presence of some ambiguous dominant energy named as dark energy (DE). To study this expansion and the concept of DE, there are two ways to modify action of GR by modifying either the matter Lagrangian or the gravitational sector. Modifications of gravitational part result in alternate gravity theories like $f(\mathscr{R})$ theory, where $\mathscr{R}$ is the Ricci scalar, $f(\mathbb{T},\tau)$, where $\mathbb{T}$ and τ are, respectively, energy-momentum tensor trace and torsion scalar, Gauss–Bonnet theory, Cartan gravity, Brans–Dicke framework, Rosen bimetric and M-theory, etc. In this respect, an interesting and significant extension of GR has been presented by Harko et al. [26], which involves a non-minimal coupling of curvature and matter field. This theory has been used in studying various cosmic aspects like thermodynamical laws, cosmological reconstruction, energy conditions, etc. [27–30]. Shabani and Farhoudi [31] elaborated the "weak field limit" by using a dynamical procedure. They analyzed the cosmological solutions of $f(\mathscr{R},\mathbb{T})$ theory by taking into account some parameters like Hubble parameter and EoS parameter. Noureen and Zubair [32] studied the instability of spherically symmetric star in $f(\mathscr{R},\mathbb{T})$ gravity in the presence of anisotropic fluid distribution.

Different approaches have been developed to formulate the analytical solutions of GR equations. One of them is to use the embedding of a four-dimensional curved spacetime into a higher-dimensional flat spacetime. Such type of embedding has proved to be a successful technique in the acquisition of several new exact models in cosmology and astrophysics [33]. Embedding approach, in fact, generates an extra differential equation establishing an interrelation between metric potentials which is known as Karmarkar condition [34]. Any valid assumption for one of the metric potentials can generate the whole solution [35, 36] and is regarded as class-I solution. Here, it is worthwhile to mention that the Schwarzschild solutions for interior and exterior geometry are of class-I and class-II, respectively [37]. In literature, numerous stellar models have been utilized to obtain different new classes of cosmologically viable embedding class-I solutions by assuming valid expressions of metric function. In this respect, various authors applied Karmarkar condition to model compact stars in the framework of GR as well as its different modified versions. Maurya and his collaborators [38–45] studied compact stars evolving under different backgrounds and developed the compact object models using Karmarkar condition. They constructed well-behaved anisotropic solutions representing realistic compact stars like Her X-1, RXJ 1856-37, LMC X-4, EXO 1785-248, 4PSR J1903 + 327, and 4 U 1820-30. However, for anisotropic matter, numerous cosmic models for different compact objects [35, 36, 41, 42, 46–54] are considered by assuming physically rational expressions of line elements to test distinctive newly defined models of realistic results in class-I embedding.

Many researchers worked on stellar modeling under Karmarkar condition [50, 51, 55]. Malaver [56] considered different forms of metric potentials to model compact star by using equation of state. Jasim et al. [57] studied a model for anisotropic fluid sphere under general relativity. Singh et al. [53] studied a new static model for anisotropic fluid distribution using Karmarkar condition in GR. Abbas et al. [58] have explored the modeling of quintessence compact stars satisfying Karmarkar condition. Naidu et al. [59] have checked the physical properties of radiating and collapsing stars using embedded class spacetime. Singh et al. [52] have also found the models of compact stars using non-flat embedded class-I spacetime. Zubair and Abbas [60] studied the interior models of some specific compact stars in the background of $f(\mathscr{R},\mathbb{T})$ gravity theory using Krori and Barua solution [61]. Zubair et al. [62] also discussed the possible formation of compact stars using spherically symmetric metric in $f(\mathscr{R},\mathbb{T})$ gravity theory. Moraes [63] investigated the "stellar equilibrium configurations" of compact stars in $f(\mathscr{R},\mathbb{T})$ gravity theory using hydrostatic equilibrium equation and also verified the physical properties of the stars. Recently, Zubair and his collaborator [64] discussed the existence of spherical compact stellar models in $f(R,T)$ theory using anisotropic matter. Some other remarkable work has been done on compact stars under modified gravity theories [65–70].

Being inspired from this literature, we shall extend these works in $f(R,T)$ theory. In this paper, we shall work on the modeling of compact star in the context of $f(\mathscr{R},\mathbb{T})$ modified theory. To pursue this, we shall assume static and spherically symmetric geometry with anisotropic distribution of matter. In Section 2, we shall define the basics of $f(\mathscr{R},\mathbb{T})$ gravity theory and present its field equations. In Section 3, we shall define the famous Karmarkar condition and present the corresponding embedding class-I solutions. Section 4 shall provide the matching of interior and exterior geometries via junction conditions and the determined values of unknown parameters. In Section 5, we shall provide the graphical analysis of the obtained model for compact star Vela X-1 against different λ. Here, we shall also check the physical stability of the achieved model. The last section shall provide a summary of major conclusions drawn.

2. Basics of $f(\mathscr{R},\mathbb{T})$ Modified Framework and Field Equations

In this section, we shall briefly define the basics of $f(\mathscr{R},T)$ theory and its field equations. The general action of the $f(\mathscr{R},\mathbb{T})$ modified gravity theories is described as [26]

$$S = \frac{1}{2\kappa^2}\int \left(f(\mathscr{R},\mathbb{T}) + \mathbb{L}_m\right)\sqrt{-g}d^4x, \tag{1}$$

where $\kappa^2 = (8\pi G/c^2)$ and herein we shall set $G = c = 1$ for further calculations. Also, the symbols L_m and $\sqrt{-g}$ represent the Lagrangian matter and determinant of metric tensor, respectively. By taking the variation of action (1) with respect to the metric tensor $(g_{\psi\varphi})$, we get the following form of field equations:

$$\mathscr{R}_{\psi\varphi} - \nabla_\psi\nabla_\varphi f_{\mathscr{R}}(\mathscr{R},\mathbb{T}) - \left[\frac{1}{2}f(\mathscr{R},\mathbb{T}) - \Box f_{\mathscr{R}}(\mathscr{R},\mathbb{T})\right]g_{\psi\varphi} = 8\pi\mathbb{T}_{\psi\varphi} - f_{\mathbb{T}}(\mathscr{R},\mathbb{T})\left(\mathbb{T}_{\psi\varphi} + \Theta_{\psi\varphi}\right), \tag{2}$$

where $\mathscr{R}_{\psi\varphi}$ represents the Ricci tensor and ∇_ψ stands for covariant derivative while $f_{\mathscr{R}}(\mathscr{R},\mathbb{T})$ and $f_{\mathbb{T}}(\mathscr{R},\mathbb{T})$ denote the derivatives with respect to Ricci scalar $\mathscr{R}$ and energy-momentum tensor trace $\mathbb{T}$, respectively. Here, the introduced terms $\Theta_{\psi\varphi}$ and $\mathbb{T}_{\psi\varphi}$ are linked with the stress-energy tensor and are defined as

$$\mathbb{T}_{\psi\varphi} = g_{\psi\varphi}\mathbb{L}_m - 2\frac{\partial\mathbb{L}_m}{\partial g^{\psi\varphi}}, \qquad \Theta_{\psi\varphi} = g^{\mu\nu}\frac{\delta\mathbb{T}_{\mu\nu}}{\delta g^{\psi\varphi}}. \tag{3}$$

It is argued that, in the framework of $f(\mathscr{R},\mathbb{T})$ theory, the tensor $\mathbb{T}_{\psi\varphi}$ does not remain conserved as compared to other modified gravity theories [71, 72] and hence gives rise to the following conservation equation:

$$\nabla^\psi\mathbb{T}_{\psi\varphi} = \frac{f_{\mathbb{T}}(\mathscr{R},\mathbb{T})}{8\pi - f_{\mathbb{T}}}(\mathscr{R},\mathbb{T})\left[\left(\mathbb{T}_{\psi\varphi} + \Theta_{\psi\varphi}\right)\nabla^\psi\ln\left(f_{\mathbb{T}}(\mathscr{R},\mathbb{T})\right) + \nabla^\psi\Theta_{\psi\varphi} - \frac{g_{\psi\varphi}}{2}\nabla^\psi\mathbb{T}\right]. \tag{4}$$

For the present work, let us assume anisotropic fluid distribution which is defined as

$$\mathbb{T}_{\psi\varphi} = (\rho + p_t)\vartheta_\psi\vartheta_\varphi - p_t g_{\psi\varphi} + (p_r - p_t)\eta_\psi\eta_\varphi, \tag{5}$$

where ϑ_ψ and η_ψ both represent the four-velocity vectors. Also, ρ denotes the matter density while p_r and p_t stand for radial and tangential pressures, respectively. For simplicity purposes, here we consider a simple and viable form of generic function $f(\mathscr{R},\mathbb{T})$ given by $f(\mathscr{R},\mathbb{T}) = f(\mathscr{R}) + f(\mathbb{T})$, where $f(\mathscr{R}) = \mathscr{R}$ and $f(\mathbb{T}) = \lambda\mathbb{T}$. Consequently, its final form can be written as

$$f(\mathscr{R},\mathbb{T}) = \mathscr{R} + \lambda\mathbb{T}. \tag{6}$$

Further, we consider the spherically symmetric spacetime representing the internal structure of static celestial object and which is given by line element:

$$ds^2 = -e^{\varphi(r)}dt^2 + e^{\phi(r)}dr^2 + r^2d\theta^2 + r^2\sin^2\theta d\phi^2, \tag{7}$$

where $e^{\varphi(r)}$ and $e^{\phi(r)}$ both represent the metric potentials. Using equation (2) along with the metric defined in equation (7), we get the following form of field equations:

$$\rho = \frac{e^{-\phi(r)}\left(r\left(2\lambda r\varphi'(r) + \lambda\varphi'(r)\left(4 - r\phi'(r)\right) + \lambda r\varphi'(r)^2 + (8\lambda+4)\phi'(r)\right) + 4(2\lambda+1)\left(e^{\phi(r)} - 1\right)\right)}{4(\lambda+1)(2\lambda+1)r^2}, \tag{8}$$

$$p_r = \frac{e^{-\phi(r)}\left(r\left(\varphi'(r)\left(\lambda(-r)\varphi'(r) + \lambda r\phi'(r) + 4\lambda + 4\right) - 2\lambda r\varphi'(r)\right) - 4(2\lambda+1)\left(e^{\phi(r)} - 1\right)\right)}{4(\lambda+1)(2\lambda+1)r^2}, \tag{9}$$

$$p_t = \frac{e^{-\phi(r)}\left(2(\lambda+1)r\varphi'(r) + \varphi'(r)\left(2 - (\lambda+1)r\phi'(r)\right) + (\lambda+1)r\varphi'(r)^2 - 2(2\lambda+1)\phi'(r)\right)}{4(\lambda+1)(2\lambda+1)r}, \tag{10}$$

$$\Delta = \frac{e^{-\phi(r)}\left(r\left(2r\varphi'(r) + \varphi'(r)\left(r\varphi'(r) - r\phi'(r) - 2\right) - 2\phi'(r)\right) + 4\left(e^{e\phi(r)} - 1\right)\right)}{4(\lambda+1)r^2}, \tag{11}$$

where Δ represents anisotropic function and is defined as $\Delta = p_t - p_r$.

3. Karmarkar Condition and Embedding Class-I Compact Star Model

In this section, we shall define the well-famed Karmarkar condition and the corresponding embedding class-I solutions in $f(R,T)$ theory. Eiesland provided [73] the necessary and sufficient condition for Riemannian space of class-I in the following form:

$$\mathcal{R}_{1414}\mathcal{R}_{2323} = \mathcal{R}_{1212}\mathcal{R}_{3434} + \mathcal{R}_{1224}\mathcal{R}_{1334}. \tag{12}$$

By using the above equation for spherically symmetric line element, it is easy to find a differential equation in terms of φ and ϕ as follows:

$$\left(\phi' - \varphi'\right)\varphi' e^{\phi} + 2\left(1 - e^{\phi}\right)\varphi' + \varphi'^{2} = 0. \tag{13}$$

The integration of equation (13) yields

$$e^{\varphi} = \left[A + B\int \sqrt{e^{\phi} - 1}\,\mathrm{d}r\right]^{2}, \tag{14}$$

where A and B are introduced as integration constants.

With the help of the above equation, one can write the anisotropy function as follows:

$$\Delta = \frac{\varphi'(r)}{4(\lambda+1)e^{\phi(r)}}\left[\frac{2}{r} - \frac{\phi'(r)}{e^{\phi(r)} - 1}\right]\left[\frac{e^{\varphi(r)}\varphi'(r)}{2B^{2}r} - 1\right]. \tag{15}$$

By imposing isotropy condition, i.e., $\Delta = 0$, it gives us three possibilities to find solutions:

(1) $e^{\varphi} = C$ and $e^{\phi} = 1$

(2) Schwarzschild interior solution

(3) Kohler-Chao cosmological solution

It is interesting to mention here that the first two solutions do not give any new and physical interesting result but the third one is a cosmological solution (as the pressure disappears at $r \longrightarrow \infty$).

Now, we shall find a compact star model filled with anisotropic fluid by taking Karmarkar condition into account. For this purpose, we assume the following form for one of the metric potentials $e^{\phi(r)}$ [74]:

$$e^{\phi(r)} = ar^{2} + b^{n-1}r^{n} + 1, \tag{16}$$

where a and b represent arbitrary constants while n is a free parameter. It is interesting to mention here that this choice of gravitational potential g_{rr} depicts finite, regular, and increasing behavior. Consequently, we get the following expression for the other metric potential:

$$e^{\varphi(r)} = \left(\frac{2B\left((n-6)\left(abr^{2} + b^{n}r^{n}\right) - ab(n-2)r^{2}J(r)\sqrt{ab^{1-n}r^{2-n} + 1}\,\right)}{b(n-6)(n+2)\sqrt{a + b^{n-1}r^{n-2}}} + A\right)^{2}, \tag{17}$$

where

$$J(r) = {}_2F_1\left(\frac{1}{2}, \frac{n-6}{2(n-2)}; \frac{10-3n}{4-2n}; -ab^{1-n}r^{2-n}\right). \tag{18}$$

Hence, the embedding class-I solution can be written as

$$\mathrm{d}s^{2} = -\left(\frac{2B\left((n-6)\left(abr^{2} + b^{n}r^{n}\right) - ab(n-2)r^{2}J(r)\sqrt{ab^{1-n}r^{2-n} + 1}\,\right)}{b(n-6)(n+2)\sqrt{a + b^{n-1}r^{n-2}}} + A\right)^{2}\mathrm{d}t^{2} + \left(ar^{2} + b^{n-1}r^{n} + 1\right)\mathrm{d}r^{2} + r^{2}\mathrm{d}\theta^{2} + r^{2}\sin^{2}\theta\mathrm{d}\phi^{2}. \tag{19}$$

Now, by using the values of both metric potentials e^{φ} and e^{ϕ} in equations (8)–(11), we get the following expressions of matter density and radial and tangential pressures, respectively:

$$\rho = \frac{b^{-n}r^{-n-2}}{2(\lambda+1)(2\lambda+1)c(r)e(r)g(r)}\left[\left(\begin{array}{c} 4abB(2\lambda+1)(n-2)r^2J(r)h(r)\left(abr^2+b^nr^n\right)-(n-6)b^nc(r)r^n\times \\ \left(4a^3b^3B(2\lambda+1)r^6+2a^2b^2r^4k(r)+2abr^2\left(2b^{n+1}r^n(A(2\lambda+1)(n+2)d(r)\right.\right. \\ \left.\left.+B(12\lambda+4\lambda n+n+4))+3b^2(n+2)(A(2\lambda+1)d(r)+B\lambda)+6B(2\lambda+1)b^{2n}r^{2n}\right) \\ +b^nm(r)r^n)\end{array}\right)\right],$$

$$p_r = \frac{b^{-n}r^{-n-2}}{2(\lambda+1)(2\lambda+1)c(r)e(r)g(r)}\left[\left((n-6)b^nc(r)r^n\left(4a^3b^3B(2\lambda+1)r^6+2a^2b^2r^4\left(Ab(2\lambda+1)(n+2)d(r)+6B(2\lambda+1)b^nr^n\right.\right.\right.$$
$$\left.\left.\left.-2bB(\lambda n+n+1))+2abr^2o(r)+b^nr^np(r)\right)-4abB(2\lambda+1)(n-2)r^2\sqrt{e(r)}J(r)\times\left(abr^2+b^nr^n\right)^2\right)\right]$$

$$p_t = \frac{r^{-n-2}}{2(\lambda+1)(2\lambda+1)c(r)e(r)g(r)}\left[\left(-b(n-6)c(r)r^n\left(2a^2b^2Br^4(n-4\lambda)+2ab(n+2)r^2s(r)+b^nr^nt(r)\right)\right.\right.$$
$$\left.\left.-2aB(2\lambda+1)(n-2)r^2b^{2-n}J(r)\left(abr^2+b^nr^n\right)\left(2abr^2+nb^nr^n\right)\right)\right]$$

$$\Delta = \frac{b^{-n}r^{-n-2}u(r)v(r)}{2(\lambda+1)c(r)e(r)g(r)}, \tag{20}$$

where

$$\begin{aligned}
c(r) &= \sqrt{ab^{1-n}r^{2-n}+1},\\
d[r] &= \sqrt{a+b^{n-1}r^{n-2}},\\
e[r] &= \left(abr^2+b^nr^n+b\right)^2,\\
u[r] &= 2a^2b^2r^4+b^{n+1}r^n\left(4ar^2-n+2\right)+2b^{2n}r^{2n},\\
l[r] &= A(2\lambda+1)(n+2)d(r)+2B(4\lambda+3\lambda n+n+1),\\
s[r] &= -Ab(2\lambda+1)d(r)+B(1-2\lambda)b^nr^n+bB(\lambda+2),\\
h[r] &= b^{n+1}r^n\left(2ar^2+n+1\right)+ab^2r^2\left(ar^2+3\right)+b^{2n}r^{2n},\\
k[r] &= Ab(2\lambda+1)(n+2)d(r)+6B(2\lambda+1)b^nr^n+2bB(\lambda(n+8)+3),\\
g[r] &= (6-n)\left(2abBr^2+Ab(n+2)d(r)+2Bb^nr^n\right)+2abB(n-2)r^2c(r)J(r),\\
m[r] &= b^2(n+2)(2A(2\lambda+1)(n+1)d(r)+B\lambda(n+4))+4B(2\lambda+1)b^{2n}r^{2n}+2b^{n+1}l(r)r^n,\\
v[r] &= (n-6)b^nc(r)r^n\left(-bB\left(-2ar^2+n+2\right)+Ab(n+2)d(r)+2Bb^nr^n\right)-2abB(n-2)\times r^2J(r)\left(abr^2+b^nr^n\right),\\
o[r] &= Ab(2\lambda+1)(n+2)d(r)\left(2b^nr^n+b\right)+B\left(6(2\lambda+1)b^{2n}r^{2n}-4b^{n+1}(\lambda n+n+1)r^n-b^2(\lambda+2)(n+2)\right),\\
p[r] &= 2Ab(2\lambda+1)(n+2)d(r)\left(b^nr^n+b\right)+B\left(4(2\lambda+1)b^{2n}r^{2n}-4b^{n+1}(\lambda n+n+1)r^n+b^2(n+2)(\lambda(n-4)-4)\right),\\
t[r] &= b(n+2)(B(\lambda n+n+2)-A(2\lambda+1)n\,d(r))-4Bb^n(\lambda n-1)r^n.
\end{aligned} \tag{21}$$

4. Evaluation of Constants Using Junction or Matching Conditions

Here, we shall determine the values of arbitrary constants present in the obtained model using junction conditions. The matching conditions play a significant role in studying stellar objects by combining the internal and external geometries on the surface of the compact object ($r = R$). These conditions ensure that crucial characteristics of stellar development are examined smoothly. We have to match

smoothly Schwarzschild metric which is taken as outer spacetime (+) with the inner spacetime (−) to attain the comprehensive set of parameters in terms of mass "M" and radius "R" of the star. The well-known Schwarzschild metric which is taken as exterior solution, for the present work, can be written as

$$ds^2 = -\zeta dt^2 + \zeta^{-1} dr^2 + r^2 d\Omega^2, \tag{22}$$

where $\zeta = (1 - 2M/R)$, $\zeta^{-1} = (1 - 2M/R)^{-1}$, and $d\Omega^2 = d\theta^2 + \sin^2\theta d\Phi^2$.

The contributions introduced by the $f(\mathscr{R}, \mathbb{T})$ model from the geometric and material sectors can significantly change the external spacetime encircling the compact object interior and even can avoid an appropriate connection by introducing unusual behaviors on the surface. In addition, vacuum approaches in the cases of modified gravity theories may or may not correlate with those of general relativity. Matching conditions also play their vital role in finding the mass 'M'' and radius 'R'' of the stellar model. In this regard, Senovilla [75] investigated the familiar Israel-Darmois [76, 77] matching conditions for $f(\mathscr{R})$ gravity theory, taking into account the distribution of isotropic and anisotropic compact materials, and claimed that, in the domain of $f(\mathscr{R})$ theory, these junction conditions are not fulfilled at all. In the framework of $f(\mathscr{R}, \mathbb{T})$ gravity theory, the presence of geometric and material modifications makes the situation more complex. In $f(\mathscr{R}, \mathbb{T})$ scenario, the matter contribution is from the trace of energy-momentum tensor $\mathbb{T}$ but the matter contribution is quite distinct from that of general relativity in which Ricci scalar $\mathscr{R}$ gives us the geometrical contribution which is coupled by the parameter λ.

It is worthy to point here that a radial coordinate condition, i.e., $r > r_s$, must be implemented for avoiding the possible finding of black hole configuration. The junction conditions for the continuity of metric components g_{tt} and g_{rr} are defined as

$$\begin{aligned} g_{tt}^{-} &= g_{tt}^{+}, \\ g_{rr}^{-} &= g_{rr}^{+}, \\ \frac{\partial g_{tt}^{-}}{\partial r} &= \frac{\partial g_{tt}^{+}}{\partial r}. \end{aligned} \tag{23}$$

By plugging all the corresponding values in equation (23), we obtain the following relations:

$$\begin{aligned} &\left(1 - \frac{2M}{R}\right) = \frac{1}{aR^2 + b^{n-1}R^n + 1}, \\ &\left(1 - \frac{2M}{R}\right) = \left(A + \frac{1}{b(n-6)(n+2)\sqrt{a + b^{n-1}R^{n-2}}}\left[2B\left[(n-6)\left(abR^2 + b^nR^n\right) - ab(n-2)R^2 J(R)\sqrt{ab^{1-n}R^{2-n} + 1}\,\right]\right]\right)^2, \\ &p_r(r = R) = 0. \end{aligned} \tag{24}$$

Here, the first two equations are linked with the external curvature continuity while the third equation is associated with the size of compact object. Due to the lack of free material substance, the continuity of the outer curvature is guaranteed, meaning that the boundary part is entirely regular and smooth. Otherwise, the presence of this material would lead to discontinuity. Using all these relations, we find the values of involved parameters as follows:

$$a = -\frac{2Mb^nR^n - b^nR^{n+1} + 2bM}{bR^2(2M - R)}, \tag{25}$$

$$A = \frac{1}{b(n-6)(n+2)\sqrt{a + b^{n-1}R^{n-2}}}\left[2abB(n-2)R^2 J(R)\sqrt{ab^{1-n}R^{2-n} + 1} + (n-6)\left(b(n+2)\times\sqrt{1 - \frac{2M}{R}}\sqrt{a + b^{n-1}R^{n-2}} - 2abBR^2 - 2Bb^nR^n\right)\right] \tag{26}$$

$$B = \frac{2(2\lambda+1)\sqrt{1 - (2M/R)}\sqrt{a + b^{n-1}R^{n-2}}\left(a^2b^2R^4 + abR^2(2b^nR^n + b) + b^nR^n(b^nR^n + b)\right)}{4a^2b^2(\lambda+1)R^4 + 2abR^2\left(4(\lambda+1)b^nR^n + b(\lambda+2)\right) + b^nR^n\left(4(\lambda+1)b^nR^n + b(4\lambda - n\lambda + 4)\right)}, \tag{27}$$

where b is a free parameter while for parameters M and R, we shall use the observed values of a well-known realistic compact star.

5. Physical Properties

In the following subsections, the physical requirements of the anisotropic stellar model will be examined graphically. For this, we take the compact star Vela X-1 into account whose mass and radius are already defined [78] and, consequently, the values of parameter A, B, and a will be calculated from equations (25)–(27). These values are summarized in the form of Table 1.

5.1. Regularity of Metric Potentials, ρ, p_r, p_t, and Δ. The graphical representation of metric potentials is provided in Figure 1 which shows that both metric components are physically acceptable; i.e., they admit regular, positive, and increasing behavior throughout surface of star for all chosen λ values. It is argued that both radial and transverse pressure components must be equal to satisfy the regularity at the center, i.e., $r = 0$, which leads to

$$p_{r0} = p_{t0} = \frac{\sqrt{a}B(\lambda+2) - a(2A\lambda + A)}{A(\lambda+1)(2\lambda+1)}, \tag{28}$$

and hence affirms the regularity at $r = 0$. Also, the central density can be described as

$$\rho = \frac{6aA\lambda + 3aA + 3\sqrt{a}B\lambda}{2A\lambda^2 + 3A\lambda + A}, \tag{29}$$

which indicates that the density behaves positively at the center.

Figure 2 shows the decreasing but positive behavior of ρ towards the outer surface of star and which has maximum value at the center, for small and large values of λ.

Further, the behavior of both pressures (radial and tangential) is shown in Figure 3 which indicates that both pressure components exhibit positive decreasing behavior from the center to the outer surface of the star. From Figure 4, the behavior of anisotropy parameter can be observed which indicates that this function vanishes at the center. It is seen that the anisotropy parameter has positive (non-vanishing) increasing behavior from the center towards the outer surface of star when small values of λ are taken into account, while, for larger values of λ, it shows negative behavior which is non-realistic. It is worthy to mention here that the non-negative condition of anisotropy parameter is completely fulfilled for $\lambda = 0.25, 0.35, 0.45$ for $0 < r < 9.69$. Further, the graphical illustration of gradients is shown in Figures 5 and 6. It is seen that the gradients of ρ, p_r, and p_t are decreasing function of r and exhibit negative behavior and, consequently, the conditions $d\rho/dr < 0, dp_r/dr < 0$, and $dp_t/dr < 0$ are satisfied for all chosen values of λ.

5.2. Energy Conditions. Some special restrictions known as energy conditions must be verified for physically valid matter fields. In the context of $f(\mathscr{R}, \mathbb{T})$ gravity theory, Chakraborty [79] verified the authenticity of the energy conditions by investigating these constraints in a general way for perfect fluid spheres. In order to examine the viability of proposed model, we shall explore these conditions, namely, null energy condition (NEC), weak energy condition (WEC), and strong energy condition (SEC), graphically which are defined as

$$\begin{aligned}
\text{NEC} &=: \rho(r) + p_r(r) \geq 0, \quad \rho(r) + p_t(r) \geq 0,\\
\text{WEC} &=: \rho(r) + p_r(r) \geq 0, \quad \rho(r) + p_t(r) \geq 0,\ \rho(r) \geq 0,\\
\text{SEC} &=: \rho(r) + p_r(r) \geq 0, \quad \rho + p_r(r) + 2p_t(r) \geq 0,\\
\text{DEC} &=: \rho(r) \geq 0, \quad \rho(r) - p_r(r) \geq 0,\ \rho(r) - p_t(r) \geq 0.
\end{aligned} \tag{30}$$

The graphical behavior of these energy conditions by taking different small and large values of λ is provided in Figure 7 which indicates that these energy conditions are satisfied throughout the star surface for all chosen values of λ.

5.3. Mass Function, Red-Shift, and Compactness Parameter. Compact stellar structure's mass to radius relation is defined as

$$m = \int 4\pi\rho r^2 dr. \tag{31}$$

For the obtained stellar system, the graphical interpretation of mass function can be seen in the left plot of Figure 8 which shows that it has regularity at the center and exhibits monotonically increasing function versus for $\lambda = 0.25, 4, 10$. Now, we define the compactness parameter of the stellar function as follows:

$$u(r) = \frac{2m(r)}{r}. \tag{32}$$

The graph of compactness parameter is provided in the right plot of Figure 8 which indicates that it exhibits positive and increasing behavior versus r for small as well as large choices of λ. The red-shift function of self-gravitating system is defined as

$$\left[A - \frac{2B\left(ab(n-2)r^2\sqrt{ab^{1-n}r^{2-n}+1}\,{}_{12}F_1\left((1/2), (n-6/2(n-2)); (10-3n/4-2n); -ab^{1-n}r^{2-n}\right) + (6-n)\left(abr^2 + b^n r^n\right)\right)}{b(n-6)(n+2)\sqrt{a+b^{n-1}r^{n-2}}}\right]^{-1} - 1. \tag{33}$$

Table 1: The determined values of constants a, A, and B using data of compact star Vela X-1. Here, we choose $\lambda = 0.25, 4, 10$ and $n = 7$.

λ	$a(\mathrm{km}^{-2})$	$b(\mathrm{km}^{-2})$	A	$B(\mathrm{km}^{-1})$	$R(\mathrm{km})$	$M/M_{\odot}$
$\lambda = 0.25$	0.006947	0.04	2.050756	0.04229	9.69	1.97
$\lambda = 4$	0.006947	0.04	3.21250	0.08066	9.69	1.97
$\lambda = 10$	0.006947	0.04	3.49503	0.0899995	9.69	1.97

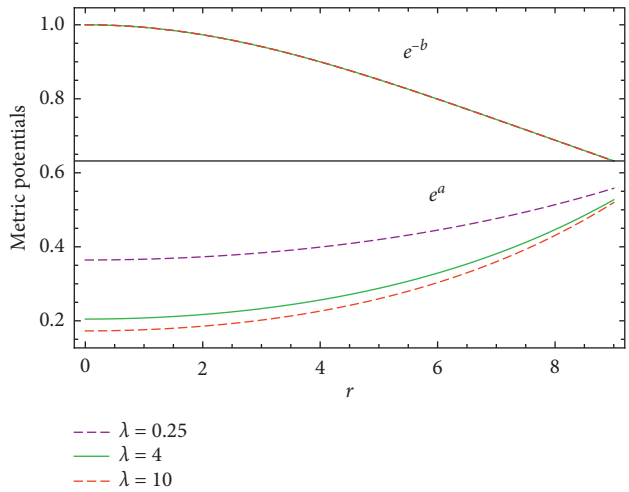

Figure 1: Behavior of e^{φ} and e^{ϕ} against r for Vela X-1 under the values of parameters from Table 1 for $\lambda = 0.25, 4$, and 10.

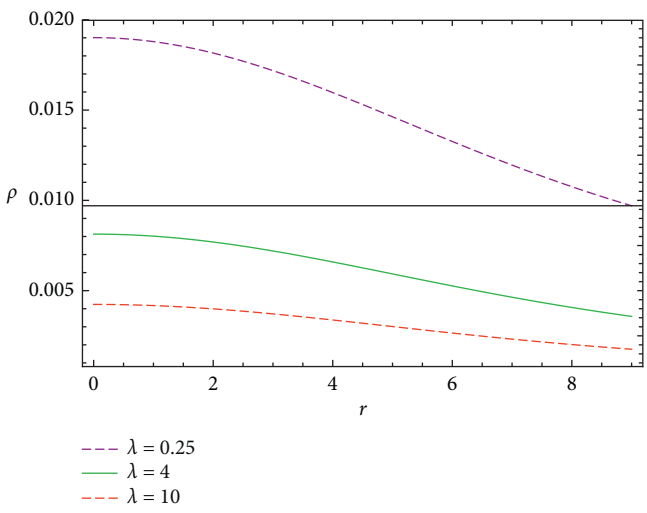

Figure 2: Behavior of ρ under one small and two large values of λ for Vela X-1.

The graphical behavior of surface red-shift function is shown in Figure 9 which indicates that it is a monotonically decreasing function of r and hence meets all physical requirements for a realistic compact.

5.4. Tolman–Oppenheimer–Volkoff (TOV) Equation or Equilibrium Condition. The non-conservative property of $f(\mathscr{R}, \mathbb{T})$ gravity gives rise to a confusion that our existing stellar model is in hydrostatic equilibrium or not. Thus, in order to make sure of proper physical conduct, the usual conservation law (identity of Bianchi) can be revised; that is,

$$\nabla^{\mu} T_{\mu\nu} = 0. \tag{34}$$

In the context of $f(\mathscr{R}, \mathbb{T})$ gravity, we acquire the TOV equation for anisotropic fluid sphere by using the above equation and which is defined as

$$\frac{-\mu'(r)}{2}(p_r + \rho) - \frac{\mathrm{d}p_r}{\mathrm{d}r} + \frac{2(p_t - p_r)}{r} = 0, \tag{35}$$

where

$$\begin{aligned} F_g &= \frac{-\mu'(r)}{2}(p_r + \rho), \\ F_h &= -\frac{\mathrm{d}p_r}{\mathrm{d}r}, \\ F_a &= \frac{2(p_t - p_r)}{r}, \end{aligned} \tag{36}$$

where F_g, F_a, and F_h represent, respectively, the force contributions coming from gravitation, anisotropy, and hydrostatic force. For a stable anisotropic configuration, the sum of all the forces must be equal to zero (as can be seen from equation (35)). Their graphical behavior of these forces depicts that anisotropic and hydrostatic forces have a combined positive effect, while the gravitational force has a repellent and dominant behavior. Hence, all three forces collectively counterbalance each other's effect and leave the stellar configuration in equilibrium state. The graphical behavior of these forces is provided in Figure 10.

5.5. Stability Condition Analysis via Causality Conditions. Here, we shall explore radial and transverse velocities of sound and the stability condition of the proposed stellar system graphically. For a stable stellar model of anisotropic configuration, the velocities should be less than 1; i.e., $v_r^2 \leq 1$ and $v_t^2 \leq 1$ [80]. These velocities are defined as

$$\begin{aligned} v_r^2 &= \frac{\mathrm{d}p_r}{\mathrm{d}r}, \\ v_t^2 &= \frac{\mathrm{d}p_t}{\mathrm{d}r}. \end{aligned} \tag{37}$$

Their plots are shown in Figure 11 which indicate that they satisfy the causality condition. Moreover, there is another method to check the stability of a compact object, known as Herrera cracking condition [6], which suggests that both potentially stable and unstable systems can be determined by taking into account some variations in the distribution of sound propagation. The difference of both

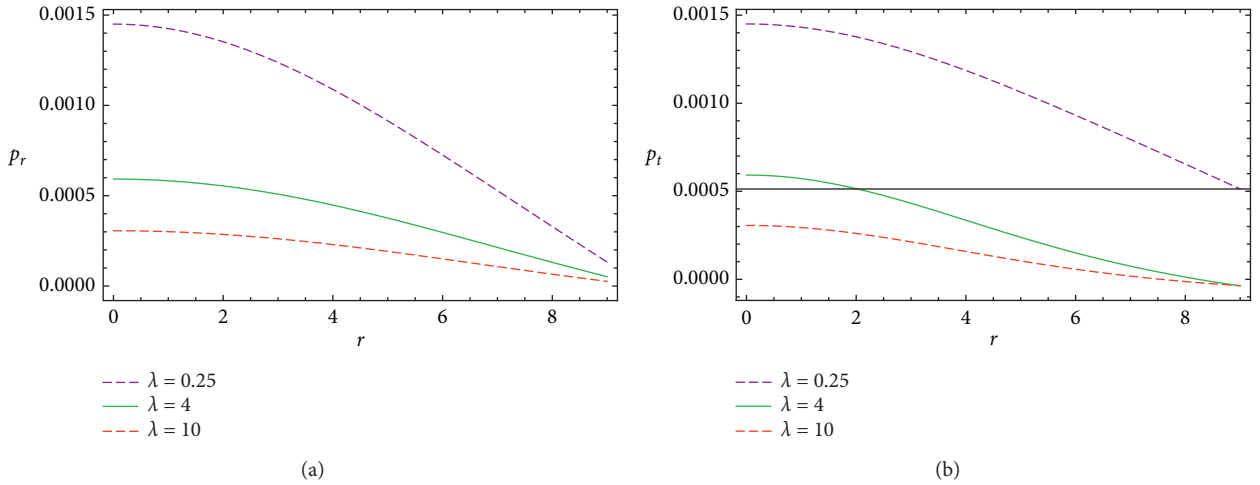

FIGURE 3: Graphical behavior of p_r and p_t against r for small and large values of λ and for values of Vela X-1 defined in Table 1.

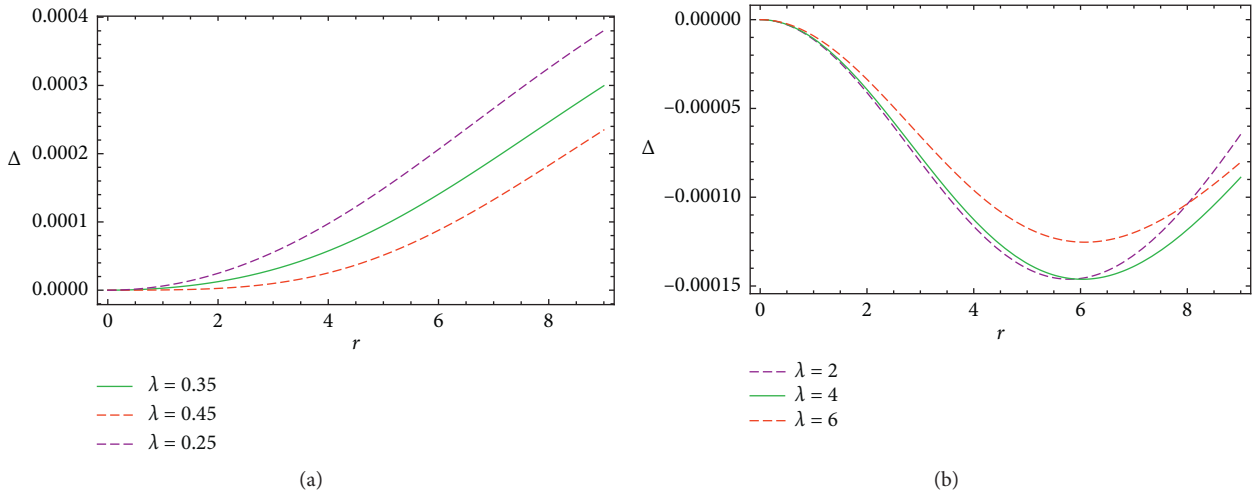

FIGURE 4: Left panel shows the graphical behavior of Δ against r for three small values: $\lambda = 0.25, 0.35, 0.45$ while right panel provides the behavior for three large values: $\lambda = 2, 4, 6$ for known values of Vela X-1 defined in Table 1.

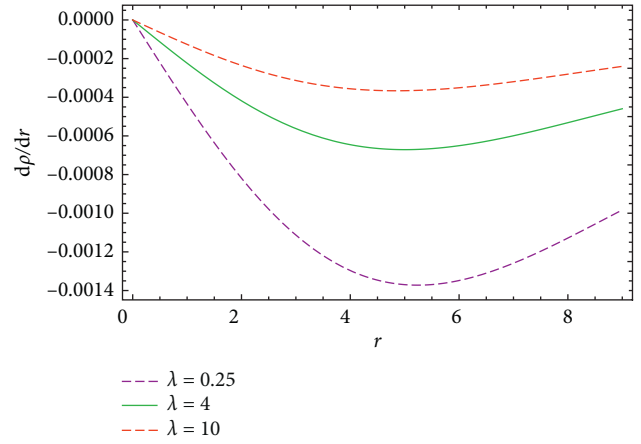

FIGURE 5: Graphical behavior of $d\rho/dr$ against r for Vela X-1 under the values of known parameters for $\lambda = 0.25, 4, 10$.

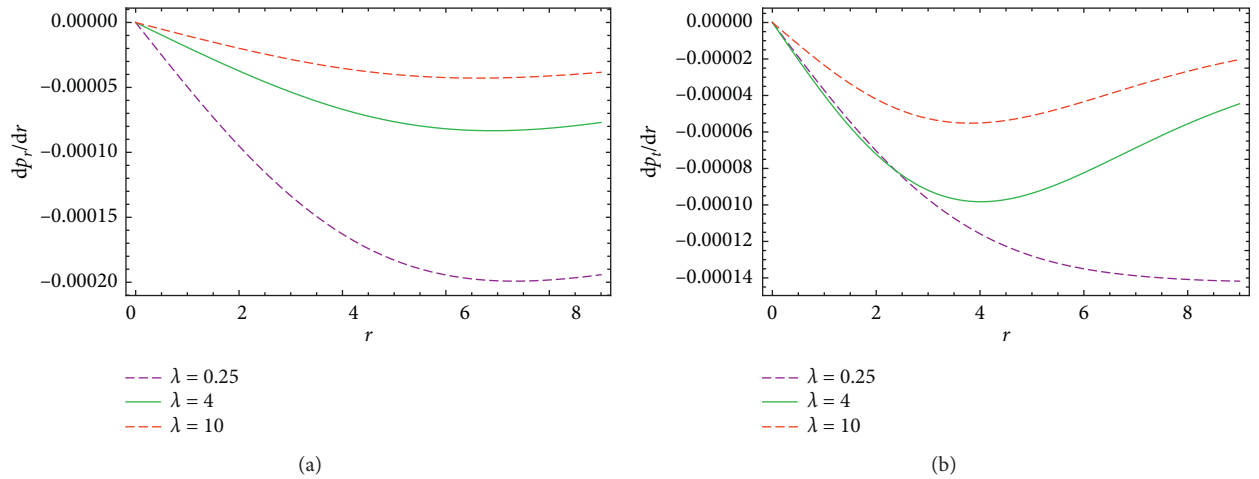

FIGURE 6: Left panel shows the behavior of $d\rho_r/dr$ against r and right panel shows the behavior of $d\rho_t/dr$ for $\lambda = 0.25, 4, 10$ for Vela X-1 star values.

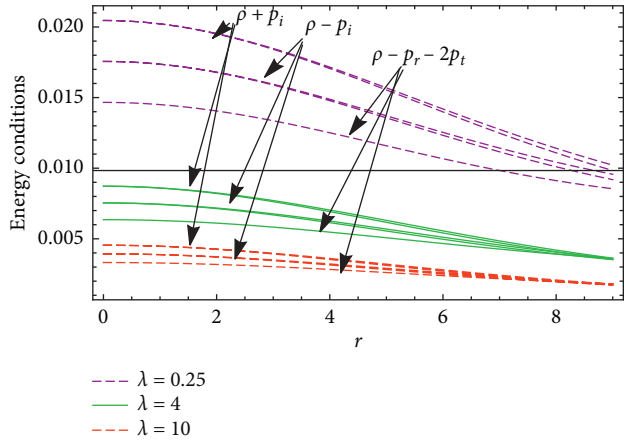

FIGURE 7: The behavior of energy conditions for different λ values: $\lambda = 0.25, 4$, and 10 for Vela X-1.

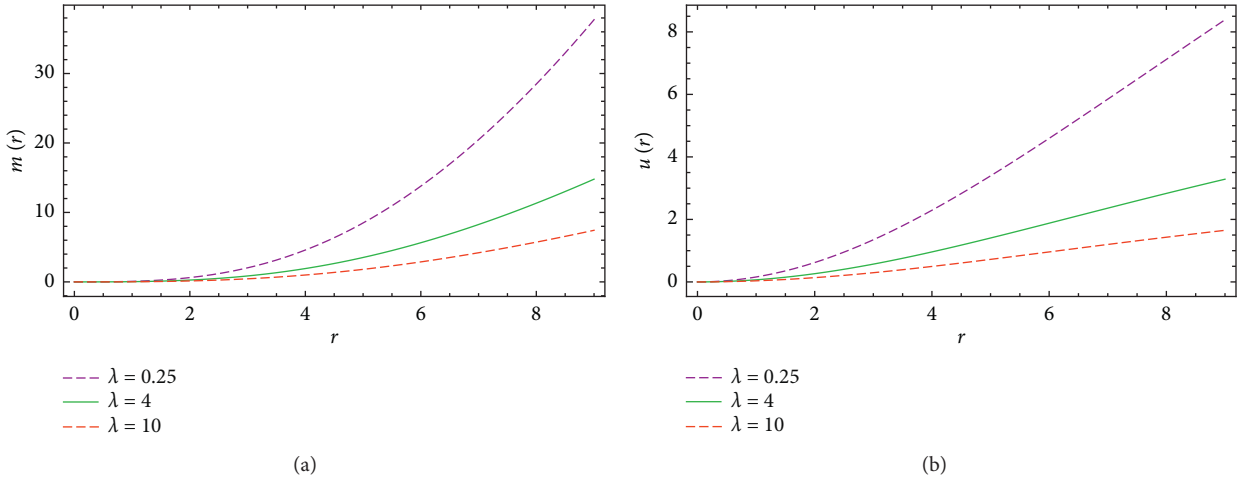

FIGURE 8: The behavior of $m(r)$ and $u(r)$ against r for Vela$X-1$ under the values of parameters from Table 1.

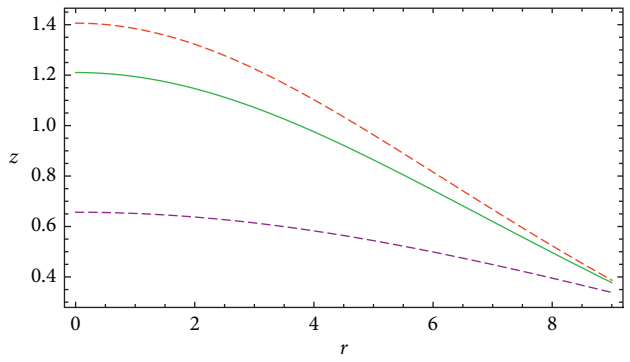

FIGURE 9: Graphical analysis of red-shift function $z(r)$ for three small and large λ values using star Vela X-1 data.

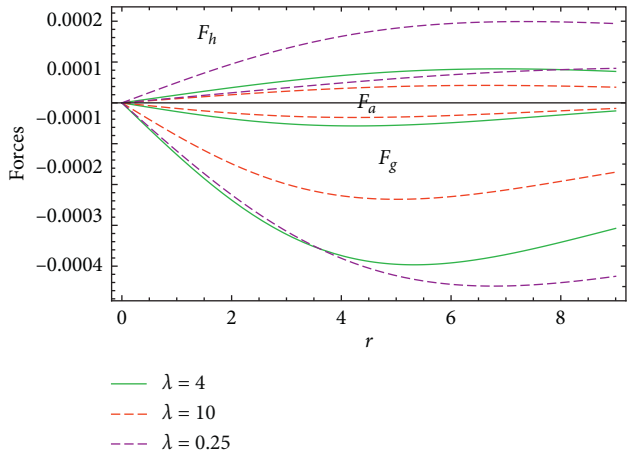

FIGURE 10: Graphical behavior of three forces, namely, F_a, F_h, and F_g, against r for Vela X-1 under the values of parameters from Table 1 with $\lambda = 0.25$, 4, and 10.

velocities $(v_t^2 - v_r^2)$ should be $-1 \le v_t^2 - v_r^2 \le 0$. The plot of Herrera cracking condition is shown in Figure 12 which indicates that the obtained stellar system satisfies this condition for small choices of λ but $v_t^2 - v_r^2$ is greater than 0 for larger λ choices.

5.6. Stability Analysis via Adiabatic Index. The adiabatic index examination is crucial for the configuration of a compact body with spherically symmetric configuration because it defines the intensity of the state equation at a defined density [81, 82]. Several researchers [60, 83] have provided the most exquisite way to examine the stability of symmetrical compact object in the face of insignificant radial adiabatic disruption by following the pioneering work of Chandrasekhar [84]. Heintzmann and Hillebrandt [85] proposed that a spherically symmetric model will be stable throughout if the condition $\Gamma > (4/3)$ holds, where Γ is the adiabatic index and is defined as

$$\Gamma = \frac{\rho + p_r}{p_r} v_r^2. \tag{38}$$

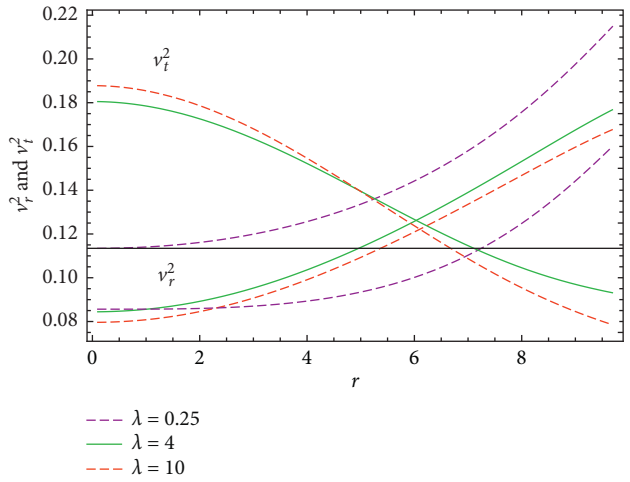

FIGURE 11: Graphical analysis of v_r^2 and v_t^2 for $\lambda = 0.25$, 4, and 10 for Vela X-1.

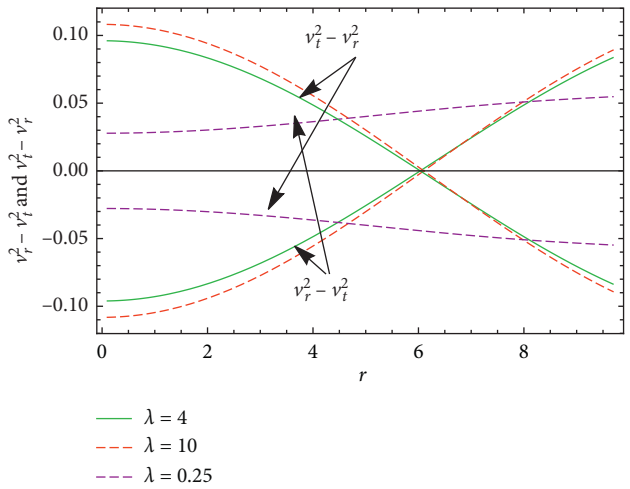

FIGURE 12: Graphical analysis of $v_t^2 - v_r^2$ and $v_r^2 - v_t^2$ for $\lambda = 0.25$, 4, and 10 for Vela X-1.

The graphical description of adiabatic index is shown in Figure 13 which shows that the stability under adiabatic index is acquired for the present model. Thus, it can be concluded that the model is stable everywhere inside the stellar object because Γ is greater than (4/3) for all chosen λ values.

5.7. Equation of State Parameter. In this subsection, we shall define and check the behavior of radial and transverse equation of state (EoS) parameters. The radial and tangential EoS parameters are defined by the following expressions:

$$\omega_r = \frac{p_r}{\rho}, \qquad \omega_t = \frac{p_t}{\rho}, \tag{39}$$

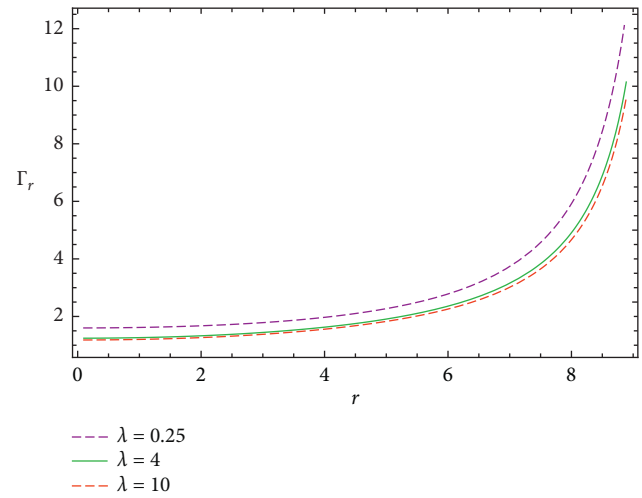

FIGURE 13: Behavior of Γ against r for Vela X-1 for different values of λ.

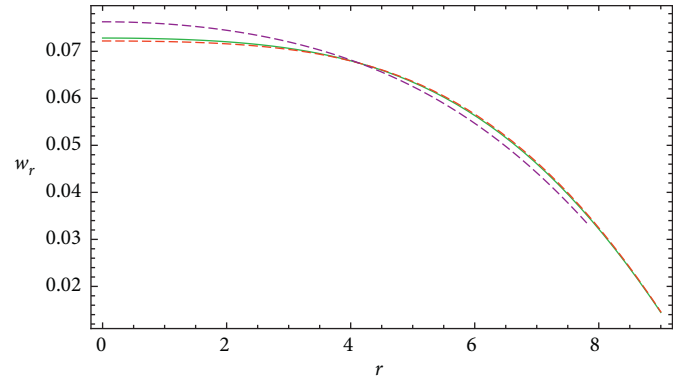

(a)

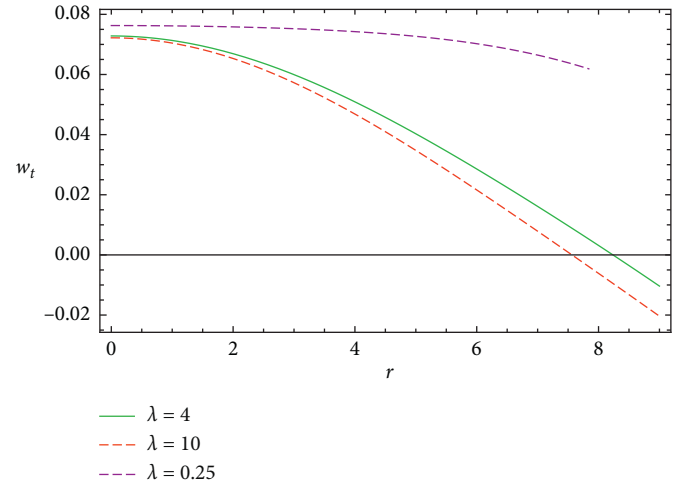

(b)

FIGURE 14: Left and right panel of the figure show the behavior of w_r and w_t, respectively, for three different values of λ and data of Vela X-1 star.

Table 2: The determined numerical values of central density, surface density, and central pressure for different values of λ. Here, we choose $\lambda = 0.25, 4, 10$.

λ	$\rho_0\,(g/\mathrm{cm}^3)$	$\rho_R\,(g/\mathrm{cm}^3)$	$p_0\,(\mathrm{dyne}/\mathrm{cm}^2)$	(p_0/ρ_0)
$\lambda = 0.25$	2.34247×10^{16}	1.31044×10^{16}	4.24437×10^{36}	0.199
$\lambda = 4$	6.24271×10^{15}	3.38795×10^{15}	1.40897×10^{36}	0.34634
$\lambda = 10$	2.85768×10^{15}	1.54579×10^{15}	6.58514×10^{35}	0.2560

where p_r and p_t denote the radial and tangential pressures while ρ denotes density of the anisotropic fluid. The graphical analysis of these parameters is provided in Figure 14 which shows that both components have monotonically decreasing behavior with respect to r. The radial and transverse components are less than 1 for the smaller choices of λ. The transverse component satisfies the condition for the range $0 \leq r \leq 7.594$ only when larger choices of λ are taken into account.

6. Concluding Remarks

In this paper, we have discussed the modeling of static, spherically symmetric stellar object filled with anisotropic matter distribution in the framework of $f(\mathscr{R}, \mathbb{T})$ theory. For obtaining closed solution to the $f(\mathscr{R}, \mathbb{T})$ dynamical equations, we have considered the simple linear form of generic function $f(\mathscr{R}, \mathbb{T})$ and utilized the well-known Karmarkar and Pandey-Sharma conditions for having embedding class-I spacetime. We have found a relationship between metric potentials e^{φ} and e^{ϕ} and then by assuming an interesting form of metric component e^{ϕ}, we have evaluated the resulting form of e^{φ} which leads to a special class of anisotropic spherical compact object. In order to check the physical validity of computed stellar solutions, one need to fix the values of involved constant parameters. For this reason, we have utilized the junction conditions across the boundary by taking Schwarzschild geometry as outer spacetime and found the values of unknown parameters which are summarized in Table 1. Here, we have applied the observed mass and radius of realistic compact star, namely, Vela X-1. For checking different physical characteristics of the constructed model, we have taken some large as well as small values of λ like $\lambda = 0.25, 4$, and 10. The numerical values of central density, surface density, and central pressure are shown in Table 2. The graphically examined essential physical properties of the proposed stellar object can be summarized as follows:

(i) The behavior of metric potentials e^{φ} and e^{ϕ} indicated that these are monotonically increasing function of r and well-behaved for all values of λ. Both components fulfill the requirement of a realistic stellar configuration.

(ii) The graphical analysis of ρ and pressure components depicted that these all are monotonically decreasing (with maximum value at the center) and positive versus r for different values of λ. Further, the graphical illustration of anisotropic function Δ showed that it is increasing radially outwards to the star surface while zero at the center, only for small choices of λ. For large λ values, anisotropic function exhibited negative behavior versus radial coordinate. It is argued that the positive Δ refers to $p_t > p_r$, which indicates the outward-directed anisotropic force while negative Δ refers to inward-directed anisotropic force. The outward-directed anisotropic force balances the gravitational force and hence corresponds to a stable realistic star configuration. Thus, in the present study, we can conclude that, for small λ choices, the anisotropic pressure is repulsive and hence supports the structure of compact object while for large λ values, it may not be stable. Further, the graphical behavior of density and pressures gradients is shown in Figures 5 and 6 which indicates that all these gradients are negative and decreasing in nature.

(iii) The graphical illustration of energy conditions indicated that these bounds are satisfied for chosen values of λ.

(iv) The behavior of mass function, compactness parameter, and red-shift function has been examined graphically. The graphical behavior of mass and compactness parameter indicated that these functions are regular, positive in nature, and gradually increasing function of r while red-shift function showed positive but decreasing behavior. It is worthy to point out here that, in our case, red-shift satisfies the Bohmer and Harko condition; i.e., $Z_s < 5$ for anisotropic matter.

(v) It has been shown that the dominating gravitational force is balanced by the combined effect of the other two forces (anisotropic and hydrostatic force) which gives us a stable configuration. Hence, our model has satisfied the Tolman–Oppenheimer–Volkoff equilibrium condition as shown graphically.

(vi) We have also examined the stability through causality condition which indicated that both radial and transverse velocities are in accordance with their respective conditions to be in equilibrium. Further, we have checked the validity of Herrera's cracking condition graphically which also confirmed the stability of our proposed stellar model.

(vii) Moreover, the stability of the stellar model has also been analyzed by the well-known adiabatic index. It can be from the graphical behavior that this

satisfied the condition, i.e., $\Gamma \geq (4/3)$, throughout the stellar evolution.

(viii) Lastly, we have explored the behavior of equation of state parameters. It has been seen that both radial and tangential parameters are less than 1 and showed decreasing behavior for all values of λ using the data of compact star Vela X-1.

From all the above discussion, it can be concluded that our defined model is stable, physically realistic, and interesting.

Data Availability

No data were used to support this study.

Conflicts of Interest

The authors declare that they have no conflicts of interest.

Acknowledgments

The authors, M. Zubair and Hina Javaid, thank the Higher Education Commission, Islamabad, Pakistan, for its financial support under the NRPU project with grant number 5329/Federal/NRPU/R&D/HEC/2016. Saira Waheed thanks Prince Mohammad Bin Fahd University, Al Khobar 31952, Saudi Arabia, for financial support.

References

[1] K. Schwarzschild, "On the gravitational field of a mass point according to Einstein's theory,"vol. 189 Sitz. Deut. Akad. Wiss. Berlin Kl. Math. Phys, 1916.

[2] K. Schwarzschild, "On the gravitational field of a sphere of incompressible fluid according to Einstein's theory," vol. 24, p. 424, 1916 Sitz. Deut. Akad. Wiss. Berlin Kl. Math. Phys.

[3] R. C. Tolman, "Static solutions of Einstein's field equations for spheres of fluid," *Physical Review*, vol. 55, no. 4, p. 364, 1939.

[4] R. C. Adams and J. M. Cohen, "Analytic stellar models in general relativity," *The Astrophysical Journal*, vol. 198, p. 507, 1975.

[5] B. Kuchowicz, "Differential conditions for physically meaningful fluid spheres in general relativity," *Physics Letters A*, vol. 38, no. 5, p. 369, 1972.

[6] L. Herrera, "Cracking of self-gravitating compact objects," *Physics Letters A*, vol. 165, no. 3, p. 206, 1992.

[7] Y. K. Gupta and M. K. Jasim, "On most general exact solution for Vaidya-Tikekar isentropicsuperdense star," *Astrophysics and Space Science*, vol. 272, no. 4, pp. 403–415, 2000.

[8] B. V. Ivanov, "Maximum bounds on the surface redshift of anisotropic stars," *Physical Review D*, vol. 65, Article ID 104011, 2002.

[9] S. D. Maharaj and M. Govender, "Behaviour of the Kramer radiating star," *Australian Journal of Physics*, vol. 50, no. 5, p. 959, 1997.

[10] H. A. Buchdahl, "General-relativistic fluid spheres. III. a static gaseous model," *The Astrophysical Journal*, vol. 147, p. 310, 1967.

[11] J. H. Jeans, "The motions of stars in a Kapteyn-universe," *Monthly Notices of the Royal Astronomical Society*, vol. 82, no. 3, p. 122, 1922.

[12] M. Ruderman, "Pulsars: structure and dynamics," *Annual Review of Astronomy and Astrophysics*, vol. 10, no. 1, p. 427, 1972.

[13] G. Lemaitre, "The expanding universe," *Annales de la Société Scientifique de Bruxelles A*, vol. 53, p. 51, 1933.

[14] A. I. Sokolov, "Phase transitions in a superfluid neutron liquid," *Journal of Experimental and Theoretical Physics*, vol. 79, p. 1137, 1980.

[15] R. F. Sawyer, "Condensedπ−phase in neutron-star matter," *Physical Review Letters*, vol. 29, no. 6, p. 382, 1972.

[16] R. L. Bowers and E. P. T. Liang, "Anisotropic spheres in general relativity," *The Astrophysical Journal*, vol. 188, p. 657, 1974.

[17] K. Dev and M. Gleiser, "Anisotropic stars: exact solutions," *General Relativity and Gravitation*, vol. 34, no. 11, p. 1793, 2002.

[18] K. Dev and M. Gleiser, "Anisotropic stars II: stability," *General Relativity and Gravitation*, vol. 35, no. 8, p. 1435, 2003.

[19] K. Dev and M. Gleiser, "Anisotropic stars: exact solutions and stability," *International Journal of Modern Physics D*, vol. 13, pp. 1389–1397, 2004.

[20] L. Herrera and N. O. Santos, "Local anisotropy in self-gravitating systems," *Physics Reports*, vol. 286, no. 2, p. 53, 1997.

[21] K. Lake, "All static spherically symmetric perfect fluid solutions of Einstein's equations," *Physical Review D*, vol. 67, Article ID 104015, 2003.

[22] L. Herrera, J. Ospino, and A. D. Prisco, "All static spherically symmetric anisotropic solutions of Einstein's equations," *Physical Review D*, vol. 77, Article ID 027502, 2008.

[23] A. G. Riess, A. V. Filippenko, P. Challis et al., "Observational evidence from supernovae for an accelerating universe and a cosmological constant," *Astronomical Journal*, vol. 116, p. 1009, 1998.

[24] P. De Bernardis, P. A. R. Ade, and N. Vittorio, "A flat Universe from high-resolution maps of the cosmic microwave background radiation," *Nature*, vol. 404, pp. 955–959, 2000.

[25] S. Perlmutter, R. A. Knop, G. Aldering et al., "New constraints on $Ω_M$, $Ω_Λ$, and w from an independent set of eleven high-redshift supernovae observed with HST," *Astrophysical Journal*, vol. 598, p. 102, 2003.

[26] T. Harko, F. S. N. Lobo, S. Nojri, and S. D. Odintsov, "$f(R, T)$ gravity," *Physical Review D*, vol. 84, Article ID 024020, 2011.

[27] M. Jamil, D. Momeni, M. Raza, and R. Myrzakulov, "Reconstruction of some cosmological models in $f(R, T)$ cosmology," *European Physical Journal C*, vol. 72, p. 1999, 2012.

[28] M. J. S. Houndjo, "Reconstruction of $f(R, T)$ gravity describing matter dominated and accelerated phases," *International Journal of Modern Physics D*, vol. 21, Article ID 1250003, 2012.

[29] F. G. Alvarenga, M. J. S. Houndjo, A. V. Monwanou, and J. B. C. Orou, "Testing some $f(R, T)$ gravity models from energy conditions," *Journal of Modern Physics*, vol. 4, pp. 130–139, 2013.

[30] M. Sharif and M. Zubair, "Thermodynamic behavior of particular $f(R, T)$-gravity models," *Journal of Experimental and Theoretical Physics*, vol. 117, pp. 248–257, 2013.

[31] H. Shabani and M. Farhoudi, "Cosmological and solar system consequences of $f(R, T)$ gravity models," *Physical Review D*.vol. 90, Article ID 044031, 2014.

[32] I. Noureen and M. Zubair, "On dynamical instability of spherical star in $f(R, T)$ gravity," *Astrophysics and Space Science*, vol. 356, no. 1, p. 103, 2015.

[33] H. Stephani, D. Kramer, M. MacCallum, C. Hoenselaers, and E. Herlt, *Exact Solution to Einstein Field Equations*, Cambridge University Press, Cambridge, England, 2003.
[34] K. R. Karmarkar, "Gravitational metrics of spherical symmetry and class one," *Proceedings of the Indian Academy of Sciences–Section A*, vol. 27, p. 56, 1948.
[35] B. V. Ivanov, "Collapsing shear-free perfect fluid spheres with heat flow," *General Relativity and Gravitation*, vol. 44, no. 7, p. 1835, 2012.
[36] B. V. Ivanov, "A conformally flat realistic anisotropic model for a compact star," *European Physical Journal C*, vol. 78, p. 332, 2018.
[37] M. Kohler and K. L. Chao, "Zentralsymmetrische statische Schwerefelder mit Räumen der Klasse 1," *Zeitschrift für Naturforschung A*, vol. 20, no. 12, p. 1537, 1965.
[38] S. K. Maurya, Y. K. Gupta, S. Ray, and S. R. Chowdhury, "Spherically symmetric charged compact stars," *European Physical Journal C*, vol. 75, p. 389, 2015.
[39] S. K. Maurya, Y. K. Gupta, S. Ray, and V. Chatterjee, "Relativistic electromagnetic mass models in spherically symmetric spacetime," *Astrophysics and Space Science*, vol. 361, p. 351, 2016.
[40] S. K. Maurya, Y. K. Gupta, T. T. Smitha, and F. Rahman, "A new exact anisotropic solution of embedding class one," *European Physical Journal A*, vol. 52, p. 191, 2016.
[41] S. K. Maurya, Y. K. Gupta, B. Dayanandan, and S. Ray, "A new model for spherically symmetric anisotropic compact star," *European Physical Journal C*, vol. 76, p. 266, 2016.
[42] P. Bhar, S. K. Maurya, Y. K. Gupta, and T. Manna, "Modelling of anisotropic compact stars of embedding class one," *European Physical Journal A*, vol. 52, p. 312, 2016.
[43] S. K. Maurya, Y. K. Gupta, S. Ray, and D. Deb, "All spherically symmetric charged anisotropic solutions for compact stars," *European Physical Journal C*, vol. 77, p. 360, 2017.
[44] S. K. Maurya and S. D. Maharaj, "Anisotropic fluid spheres of embedding class one using Karmarkar condition," *European Physical Journal C*, vol. 77, p. 328, 2017.
[45] S. K. Maurya, B. S. Ratanpal, and M. Govender, "Anisotropic stars for spherically symmetric spacetimes satisfying the Karmarkar condition," *Annals of Physics*, vol. 382, p. 36, 2017.
[46] K. Komathiraj and S. D. Maharaj, "Classes of exact Einstein-Maxwell solutions," *General Relativity and Gravitation*, vol. 39, no. 12, p. 2079, 2007.
[47] P. Bhar and M. H. Murad, "Relativistic compact anisotropic charged stellar models with Chaplygin equation of state," *Astrophysics and Space Science*, vol. 361, p. 334, 2016.
[48] F. Rahman, K. Chakraborty, P. K. F. Kuhfittig, G. C. Shit, and M. Rahman, "A new deterministic model of strange stars," *European Physical Journal C*, vol. 74, p. 3126, 2014.
[49] M. Malaver, "Strange quark star model with Quadratic equation of state," *Frontiers of Mathematics and its Applications*, vol. 1, pp. 9–11, 2014.
[50] K. N. Singh, N. Pant, and N. Pradhan, "Charged anisotropic Buchdahl solution as an embedding class I spacetime," *Astrophysics and Space Science*, vol. 361, p. 173, 2016.
[51] K. N. Singh, P. Bhar, and N. Pant, "A new solution of embedding class I representing anisotropic fluid sphere in general relativity," *International Journal of Modern Physics D*, vol. 25, no. 14, Article ID 1650099, 2016.
[52] K. N. Singh, P. Bhar, F. Rahaman, N. Pant, and M. Rahaman, "Conformally non-flat spacetime representing dense compact objects," *Modern Physics Letters A*, vol. 32, no. 18, Article ID 1750093, 2017.
[53] K. N. Singh, N. Pant, and M. Govender, "Physical viability of fluid spheres satisfying the Karmarkar condition," *European Physical Journal C*, vol. 77, p. 100, 2017.
[54] P. Bhar, K. N. Singh, and T. Manna, "A new class of relativistic model of compact stars of embedding class I," *International Journal of Modern Physics D*, vol. 26, no. 9, Article ID 1750090, 2017.
[55] T. Singh, R. Chaubey, and A. Singh, "Bouncing cosmologies with viscous fluids," *Astrophysics and Space Science*, vol. 361, p. 106, 2016.
[56] M. Malaver, "Relativistic modeling of Quark stars with Tolman IV type potential," *International Journal of Modern Physics and Application*, vol. 2, pp. 1–6, 2015.
[57] Jasim, "Generalized exact solution for a spherical symmetric perfect fluid model of embedding class two," *Applied Mathematical Sciences*, vol. 5, no. 16, pp. 763–774, 2011.
[58] G. Abbas, S. Qaisar, W. Javed, and W. Ibrahim, "Quintessence compact stars satisfying Karmarkar condition," *Canadian Journal of Physics*, vol. 97, no. 4, p. 374, 2019.
[59] N. F. Naidu, M. Govender, and S. D. Maharaj, "Radiating star with a time-dependent Karmarkar condition," *European Physical Journal C*, vol. 78, p. 48, 2018.
[60] M Zubair and G Abbas, "Some interior models of compact stars in f(R) gravity," *Astrophysics and Space Science*, vol. 361, p. 342, 2016.
[61] G. J. G. Junevicus, "An analysis of the Krori-Barua solution," *Journal of Physics A: Mathematical and General*, vol. 9, no. 12, p. 2069, 1976.
[62] M. Zubair, G. Abbas, and I. Noureen, "Possible formation of compact stars in *f(R,T)* gravity," *Astrophysics and Space Science*, vol. 36, p. 8, 2016.
[63] P. H. R. S. Moraes, J. D. V. Arbañil, and M. Malheiro, "Stellar equilibrium configurations of compact stars inf (*R*, *T*) theory of gravity," *Journal of Cosmology and Astroparticle Physics*, vol. 2016, no. 6, p. 005, 2016.
[64] G. Mustafa, M. Zubair, S. Waheed, and T. Xia, "Realistic stellar anisotropic model satisfying Karmarker condition in *f* (*R*, *T*) gravity," *European Physical Journal C*, vol. 80, p. 26, 2020.
[65] G. Abbas and H. Nazar, "Stellar shear-free gravitational collapse with Karmarkar condition in *f(R)* gravity," *International Journal of Modern Physics A*, vol. 34, Article ID 19502208, 2019.
[66] R. Ahmed and G. Abbas, "Non-adiabatic gravitational collapse in *f* (*R*, *T*) gravity with Karmarkar condition for anisotropic fluid," *Modern Physics Letters A*, vol. 35, Article ID 2050103, 2020.
[67] H. Nazar and G. Abbas, "Charged anisotropic collapsing stars with heat flux in *f* (*R*) gravity," *Chinese Journal of Physics*, vol. 63, pp. 436–447, 2020.
[68] G. Abbas and H. Nazar, "Hybrid star model with quark matter and baryonic matter in minimally coupled *f* (*R*) gravity," *Annals of Physics*, vol. 424, Article ID 168336, 2020.
[69] M. R. Shahzad and G. Abbas, "Models of quintessence compact stars in Rastall gravity consistent with observational data," *The European Physical Journal Plus*, vol. 135, pp. 1–17, 2020.
[70] R. M. Shahzad and G. Abbas, "Hybrid compact stars model in Rastall gravity: a comparative study," *Astrophysics and Space Science*, vol. 365, pp. 1–17, 2020.
[71] H. Yu, W.-D. Guo, K. Yang, and Y.-X. Liu, "Scalar particle production in a simple Horndeski theory," *Physival Review D*, vol. 97, Article ID 083524, 2018.

[72] Y. Y. Zhao, Y. B. Wu, J.-B. Lu, Z. Zhang, W.-L. Han, and L.-L. Lin, "Modified $f(G)$ gravity models with curvature–matter coupling," *European Physical Journal C*, vol. 72, p. 1924, 2012.
[73] J. Eiesland, "The group of motions of an Einstein space," *Transactions of the American Mathematical Society*, vol. 27, no. 2, p. 213, 1925.
[74] K. N. Singh, "A generalized Finch–Skea class one static solution," *The European Physical Journal C*, vol. 79, no. 5, p. 381, 2019.
[75] J. M. M. Senovilla, "Junction conditions for $F(R)$-gravity and their consequences," *Physical Review D*, vol. 88, Article ID 064015, 2013.
[76] W. Israel, "Singular hypersurfaces and thin shells in general relativity," *Il Nuovo Cimento B Series 10*, vol. 44, no. 1, p. 1, 1966.
[77] G. Darmois, "Les équations de la gravitation einsteinienne," *Mémorial des Sciences Mathematiques*, no. 27, p. 58, 1927.
[78] T. Gangopadhyay, S. Ray, X.-D. Li, J. Dey, and M. Dey, "Strange star equation of state fits the refined mass measurement of 12 pulsars and predicts their radii," *Monthly Notices of the Royal Astronomical Society*, vol. 431, no. 4, p. 3216, 2013.
[79] S. Chakraborty, "An alternative $f(R, T)$ gravity theory and the dark energy problem," *General Relativity and Gravitation*, vol. 45, no. 10, p. 2039, 2013.
[80] H. Abreu, H. Hernández, and L. A. Núñez, "Sound speeds, cracking and the stability of self-gravitating anisotropic compact objects," *Classical and Quantum Gravity*, vol. 24, no. 18, p. 4631, 2007.
[81] B. K. Harrison, K. S. Thorne, M. Wakano, and J. A. Wheeler, *Gravitation Theory and Gravitational Collapse*, University of Chicago Press, Chicago, IL, USA, 1965.
[82] P. Haensel, A. Y. Potekhin, and D. G. Yakovlev, *Neutron Stars 1: Equation of State and Structure*, Springer, Berlin, Germany, 2007.
[83] D. Horvat, S. Iliji, and A. Marunovi, "Radial pulsations and stability of anisotropic stars with quasi-local equation of state," *Classical and Quantum Gravity*, vol. 28, Article ID 025009, 2011.
[84] S. Chandrasekhar, "Dynamical instability of gaseous masses approaching the schwarzschild limit in general relativity," *Physical Review Letters*, vol. 12, no. 4, p. 114, 1964.
[85] H. Heintzmann and W. Hillebrandt, "Neutron stars with an anisotropic equation of state: mass, redshift and stability," *Astronomy & Astrophysics*, vol. 38, pp. 51–55, 1975.